Published in final edited form as:

Nat Struct Mol Biol. 2013 July ; 20(7): 789–795. doi:10.1038/nsmb.2606.

Homeostatic control of Argonaute stability by microRNA availability

Peter Smibert[1,4], **Jr-Shiuan Yang**[1,4], **Ghows Azzam**[2,3,4], **Ji-Long Liu**[2], and **Eric C. Lai**[1]

[1]Department of Developmental Biology, Sloan-Kettering Institute, New York, New York, USA.

[2]Medical Research Council Functional Genomics Unit, Department of Physiology, Anatomy and Genetics, University of Oxford, Oxford, United Kingdom.

Abstract

Homeostatic mechanisms regulate the abundance of many small RNA components. We used *Drosophila* and mammalian systems to demonstrate a conserved homeostatic system in which the status of miRNA biogenesis controls Argonaute protein stability. Clonal analyses of multiple mutants of core *Drosophila* miRNA factors revealed that stability of the miRNA effector AGO1 is dependent on miRNA biogenesis. Reciprocally, ectopic transcription of miRNAs within *in vivo* clones induced accumulation of AGO1, as did genetic interference with the ubiquitin-proteasome system. In mammals, we found that the stability of mAgo2 declined in *Dicer* knockout cells, and was rescued by proteasome blockade or introduction of either Dicer plasmid or Dicer-independent miRNA constructs. Importantly, Dicer-dependent miRNA constructs generated pre-miRNAs that bind Ago2, but did not rescue Ago2 stability. We conclude that Argonaute levels are finely tuned by cellular availability of mature miRNAs and the ubiquitin-proteasome system.

Introduction

Argonaute proteins are the effectors of diverse modes of small RNA-mediated gene silencing, and are guided to appropriate targets by their associated small RNAs[1]. Major Argonaute clients include ~22 nucleotide (nt) microRNAs (miRNAs) and ~21 nt small interfering RNAs (siRNAs) that associate with particular members of the Ago-clade subfamily, and ~24–30 nt Piwi-interacting RNAs (piRNAs) that associate with the Piwi-clade subfamily of Argonautes. Much remains to be understood about piRNA biogenesis, but the generation of miRNAs and siRNAs is relatively well-documented[2]. siRNAs generally derive from cleavage of double-strand RNAs by the Dicer RNase III enzyme into siRNA duplexes that load into Argonautes, followed by maturation into a single-stranded

Correspondence should be addressed to J.L. (jilong.liu@dpag.ox.ac.uk) or E.C.L. (laie@mskcc.org.

[3]Present address: Weatherall Institute of Molecular Medicine, University of Oxford, John Radcliffe Hospital, Oxford, United Kingdom.

[4]These authors contributed equally.

Author Contributions

P.S., J.Y. and E.L. conceived and planned the project with crucial input from G.A. and J.L. P.S., G.A. and J.L. carried out the *Drosophila* experiments and J.Y. carried out the mammalian experiments. P.S., J.Y, and E.L. wrote the text with input from G.A. and J.L.

siRNA:Argonaute complex. Primary miRNA transcripts contain hairpins that are excised by the nuclear RNase III Drosha and its double-stranded RNA binding partner DGCR8 (known as Pasha in invertebrates). The resulting pre-miRNA hairpins are then cleaved in the cytoplasm by Dicer into miRNA/star duplexes that load Argonautes and mature into single-stranded form. In addition, a variety of non-canonical pathways generate functional miRNAs independently of Drosha and/or Dicer, by exploiting diverse RNases that normally mature other types of transcripts[3]. siRNA function is mediated by the cleavage activity of *Drosophila* AGO2 and vertebrate Ago2, whereas miRNA function requires the Argonaute partner GW182, which associates with *Drosophila* AGO1 and all four vertebrate Ago-class Argonautes[4].

Homeostatic and feedback mechanisms coordinate levels of miRNAs with their effector proteins, or harmonize the level of small RNA biogenesis factors that function within complexes[5]. For example, in vertebrates and flies, an elegant feedback loop normalizes levels of Drosha and DGCR8[6–8]. *DGCR8* transcripts are destabilized by 5' hairpins that are directly cleaved by Drosha, while DGCR8 protein is reciprocally unstable in the absence of Drosha. These cross-regulatory interactions maintain appropriate stoichiometry of the Drosha–DGCR8 complex. Further studies in plant[9,10] and animal[11–13] systems uncovered requirements for the Hsp90 machinery in Argonaute loading and/or stability. Hsp90–co-chaperone complexes also facilitate loading of Piwi proteins[14], and loss of piRNA biogenesis components results in cell-autonomous loss of Piwi protein[15].

Despite these accumulating links of small RNA biogenesis pathways to the stability of their effector Argonautes, multiple previous studies did not apparently reveal alteration of the *Drosophila* miRNA effector AGO1 upon depletion of miRNA biogenesis factors in cultured S2 cells[16–19]. We re-evaluated this in the animal using null mutant clones of *drosha*, *pasha*, and *dicer-1*, all of which demonstrate reduction of AGO1. We show that AGO1 is degraded by the ubiquitin-proteasome system in the animal, and AGO1 is detectably stabilized by transgenic expression of miRNAs, demonstrating a homeostatic mechanism. We extend these findings to mammals, since Ago2 exhibits lower stability in *Dicer*-knockout cells. We could rescue Ago2 stability by inhibiting the proteasome or by introducing Dicer-independent *mir-451*-type constructs. Importantly, non-cleavable *pre-mir-451* hairpins associated with Ago2 but did not rescue its stability, indicating that the active miRISC and not simply RNA-associated Argonaute is protected from degradation. The deep conservation of a strategy by which Argonaute protein levels are sensitive to miRNA availability reflects its importance for appropriate miRNA effector function.

Results

In vivo stability of fly AGO1 depends on miRNA biogenesis

Tests from several different laboratories, albeit usually conducted for other reasons, have not revealed substantial alteration of miRNA effector AGO1 protein level upon knockdown of any miRNA biogenesis factors[16–19]. Having generated a panel of mutants in core miRNA factors[8,20], we evaluated whether AGO1 protein was sensitive to miRNA biogenesis in the animal. We generated homozygous mutant ovarian germline clones using the Flp-FRT system, which negatively marked mutant cells by absence of GFP. We stained these with

specific AGO1 antibodies[20], which in ovaries bearing control germline clones detects somatic and germline expression, with higher levels in the oocyte (Fig. 1a). As expected, germline clones of *AGO1* mutants showed decreased staining (Fig. 1a). Strikingly, germline clones of *pasha* and *dicer-1* similarly showed reduction of AGO1 protein (Fig. 1a), and analysis of three additional *dicer-1* alleles yielded similar results (Supplementary Fig. 1).

We confirmed these findings in somatic tissues, and used the mosaic analysis with a repressible cell marker (MARCM) system to positively mark mutant clones with GFP. While control wing imaginal disc MARCM clones did not show alteration of AGO1 levels (Figure 1b), clones bearing null alleles of *pasha*, *drosha*, and *dicer-1* were all strongly deficient for AGO1 protein (Figure 1b). In addition, clonal analysis of two *pasha* mutants and six *dicer-1* mutants in larval brain lobes all exhibited decreased AGO1 staining (Supplementary Fig. 2). Therefore, accumulation of the miRNA effector AGO1 depends on miRNA biogenesis, in diverse tissues and developmental stages.

A previous report did not reveal alteration of AGO1 protein level upon depletion of its cofactor GW182 in S2 cells[19]. As GW182 is encoded on chromosome 4, which is not amenable to mitotic recombination, we utilized a *GW182-RNAi* transgene. We validated that expression of this transgene reduces GW182 protein cell-autonomously (Fig. 1c) and de-represses the endogenous miRNA target Mei-P26[8,21] to similar levels seen in *pasha*, *drosha*, and *dicer-1* clones (Supplementary Fig. 3a). Interestingly, depletion of GW182 caused AGO1 protein to accumulate (Fig. 1c). This was unexpected given that mammalian GW182 was reported to protect exogenously transfected miRNAs from exonucleolytic degradation[22].

Mei-P26 is an E3 ubiquitin ligase that binds AGO1 and regulates miRNA levels[23]. However, as mutant clones of *drosha*, *pasha*, *dicer-1*, and *GW182* all deregulate Mei-P26, but only *GW182* mutant cells increase AGO1, we inferred that Mei-P26 was unlikely to be a major determinant of AGO1 stability in imaginal discs. We confirmed this by showing that while clones that misexpress Mei-P26 exhibit compromised growth[21], they maintain relatively normal levels of AGO1 (Supplementary Fig. 3b). The opposing effects of loss of core miRNA biogenesis factors and the loss of *GW182* on AGO1 accumulation provided an opportunity for *in vivo* epistasis analysis. We generated MARCM clones that were simultaneously homozygous for a null allele of *dcr-1* and expressed *GW182-RNAi* and GFP. These clones clearly displayed the AGO1 protein loss phenotype (Figure 1c), demonstrating that accumulation of AGO1 upon GW182 loss is strictly dependent on active miRNA biogenesis.

Post-transcriptional control of AGO1 stability

With knowledge of these *in vivo* data, we re-assessed the situation in *Drosophila* S2 cells. Although previous studies confirmed efficient depletion of target proteins and/or accumulation of miRNA precursors, perusal of the literature indicates difficulty of fully depleting mature miRNAs by knockdown of miRNA biogenesis components[18,24–26]. We utilized a double knockdown strategy (2x4 days soaking with dsRNA) for maximal efficacy. These trials yielded strong loss of AGO1 protein upon knockdown of *drosha*, *pasha*, and

dicer-1, compared to untreated cells or control *GFP* dsRNA (Fig. 2a). In contrast, knockdown of *GW182* reproducibly increased AGO1 levels (Fig. 2a).

These effects were paralleled by the behaviour of endogenous miR-34, levels of which were strongly decreased upon knockdown of miRNA biogenesis factors and mildly increased upon *GW182* knockdown (Fig. 2b). The latter data may potentially imply that AGO1 turnover is altered when the effector complex is disrupted. A population of mature miR-34 was maintained in *AGO1* knockdown cells despite near absence of AGO1; these species exhibited altered length profile (Fig. 2b) and likely reflected sorting to AGO2. We tested independent *AGO1* amplicons and observed no reproducible alteration of *AGO1* transcripts following knockdown of miRNA biogenesis factors (Fig. 2c), suggesting a post-transcriptional mechanism. This was supported by similar *AGO1* transcript levels in homozygous *pasha* larvae compared to wild-type (Fig. 2d).

Overall, our ability to recapitulate phenotypes from mutant clones with S2 cell knockdowns demonstrated that positive regulation of AGO1 stability by miRNA biogenesis is a general phenomenon, and appears to act post-transcriptionally.

RNAi effector AGO2 is not dependent on siRNA biogenesis

Given these results, we investigated whether the RNAi effector AGO2 was sensitive to siRNA biogenesis. We introduced a FLAG-HA-AGO2 genomic transgene that supports full RNAi function[26,27] into the *dcr-2[L811fsX]* homozygous mutant background, which lacks siRNA biogenesis capacity and RNAi capacity[28], and confirmed genotypes by PCR (Fig. 2e). We extended our previous studies[27] by showing that AGO2 protein levels were unaltered in *dcr-2* null ovaries and heads (Fig. 2f). Therefore, although both AGO1 and AGO2 are loaded using Hsp90-dependent mechanisms[11,12], the miRNA effector AGO1 is uniquely subject to turnover in the unloaded state.

Increasing miRNA transcription can stabilize AGO1 *in vivo*

We reciprocally asked whether overproduction of miRNAs could influence AGO1 levels. Imaginal disc clones expressing DsRed or different individual UAS-miRNA transgenes did not reveal substantial effects on AGO1 protein levels (Fig. 3a). However, expression of a 3-miRNA cluster (*mir-12, mir-283, mir-304*) and 4-miRNA cluster (*mir-9c, mir-79, mir-9b, mir-306*), both resulted in clear cell-autonomous accumulation of AGO1 protein (Fig. 3b). The strongest effects were seen in clones expressing the 8-miRNA cluster containing *mir-309, mir-3, mir-286, mir-4, mir-5, mir-6-1, mir-6-2, mir-6-3* (Fig. 3b). Thus, increasing AGO1 levels correlated with the number of ectopically expressed miRNAs. In contrast, clonal overexpression of an RNAi trigger to generate ectopic siRNAs (*shep-RNAi*) did not alter AGO1 (Fig. 3c). This was consistent with the bulk sorting of siRNAs into the *Drosophila* RNAi effector, AGO2.

We also analyzed the effect of ectopic miRNAs in the ovary. Similar to imaginal discs, ectopic expression of *mir-124*, but not a non-processed mutant *mir-124* construct, elevated AGO1 in ovarian follicle cells (Fig. 3d). Altogether, these data fulfil a homeostatic

mechanism in that loss and gain of miRNA biogenesis induce reciprocal effects on AGO1 accumulation.

The ubiquitin-proteasome system limits AGO1 accumulation

We hypothesized that the ubiquitin-proteasome system might mediate AGO1 homeostasis. We exploited a transgene encoding a dominant temperature sensitive subunit of the proteasome (*UAS-DTS5*), which we expressed along the anterior-posterior boundary of the wing imaginal disc using *ptc-Gal4* (Fig. 3e). We introduced an *hs-AGO1* transgene in the genetic background, so that we could monitor the outcome of a pulse of AGO1 expression across a timecourse, comparing wild-type cells with neighboring cells in which proteasome activity was impaired. Following a 15-minute heat-shock, AGO1 protein levels were greatly elevated throughout the disc, with further accumulation within the DTS5-expressing domain (Fig. 3e). Four hours after induction, the levels of AGO1 returned to normal endogenous levels throughout the disc, except within the DTS5-expressing domain (Fig. 3e). These data demonstrate that exogenous AGO1 is rapidly turned over by a proteasome-dependent mechanism.

We complemented these tests by assessing if endogenous AGO1 is regulated by ubiquitination. We were unable to recover imaginal disc clones expressing an RNAi transgene to the sole ubiquitin activating enzyme *Uba1* (data not shown), likely due to cell competition or cell lethality. However, we could recover such clones in the ovarian follicular epithelium, and these clones super-accumulated AGO1 protein (Fig. 3f). Therefore, endogenous AGO1 protein is restricted by ubiquitination.

Stability of mammalian Ago2 depends on miRNA availability

We sought to extend these findings to mammalian cells. An excellent model is a stable *Dicer*$^{-/-}$ mouse embryonic fibroblast (MEF) cell line that we have extensively characterized[29]. Although Western analysis detected endogenous mouse Ago2 (mAgo2) protein in these cells, time course analyses following cycloheximide (CHX) treatment showed that mAgo2 was destabilized in *Dicer*$^{-/-}$ cells (Fig. 4a). We assessed whether mAgo2 accumulation was sensitive to the restoration of endogenous miRNA biogenesis. Transfection of *Dicer*$^{-/-}$ cells with a FLAG-Dicer construct strongly rescued processing of endogenous let-7a into mature miRNAs (Fig. 4b). Concomitant with this, we indeed observed that completion of miRNA biogenesis substantially increased Ago2 stability (Fig. 4c).

We attempted to assess mAgo1, but did not detect its endogenous accumulation in *Dicer*$^{-/-}$ cells (Supplementary Fig. 4a). As an alternative, we transfected myc-hAgo1 into *Dicer*$^{-/-}$ cells and observed that its decay was slower than endogenous mAgo2 (Supplementary Fig. 4b). However, myc-hAgo2 did not recapitulate the instability of mAgo2. Moreover, transfection of either construct impaired the decay of endogenous mAgo2 (Supplementary Fig. 4b). We infer that this may reflect the recruitment of ectopic and endogenous Ago proteins into aggregates[30], whose loading potential and stability control might be altered. We therefore concentrated our further studies on endogenous mAgo2.

mAgo2 transcript levels in *Dicer*$^{-/-}$ cells were unaltered by CHX or FLAG-Dicer plasmid (Fig. 4d), pointing to regulation of mAgo2 protein stability. Analogous to genetic manipulations of the *Drosophila* proteasome, addition of the proteasome inhibitor MG132 suppressed mAgo2 protein decay in *Dicer*$^{-/-}$ cells treated with CHX (Fig. 4e). Given the recent report that autophagy regulates Argonaute levels in mammalian cells[31], we also treated *Dicer*$^{-/-}$ cells with the autophagy inhibitor Bafilomycin A1. This did not perturb mAgo2 levels during a 2–6 hour timecourse, even though we confirmed strong inhibition of autophagy by accumulation of LC3-II at all timepoints (Supplementary Fig. 5a). Moreover, Bafilomycin A1 did not rescue the instability of AGO1 in *Drosophila* S2 cells depleted of various miRNA biogenesis factors (Supplementary Fig. 5b). Double treatments suggested a mild stabilizing effect of Bafilomycin A1 in *Dicer*$^{-/-}$ cells beyond the effect of MG132 (Supplementary Fig. 5c). However, we were cautious to interpret this as a parallel pathway, given the possibility of indirect effects in this triple drug treatment. Interestingly, we could also improve Ago2 stability in *Dicer*$^{-/-}$ cells just by transfecting them with synthetic siRNAs (Fig. 4f). Similar findings were reported that synthetic siRNAs stabilize mammalian Argonautes in the presence of Hsp90 inhibitors[13]. These observations implied that RNA-loaded mAgo2 is more resistant to degradation.

Genetic rescue of mAgo2 stability in *Dicer* knockout cells

We tested cellular strategies to rescue miRNA biogenesis in *Dicer* cells. Vertebrate miR-451 matures via a Dicer-independent mechanism that involves direct loading of its short pre-miRNA hairpin into Ago2, followed by slicing of the complementary strand and resection of its 3' end[32]. We subsequently showed that functional miR-451 could be efficiently expressed in a Drosha and Dicer-independent fashion using a *tRNA-mir-451* fusion[33]. We exploited this as a genetic strategy to express mature miRNAs from a nuclear context in *Dicer*$^{-/-}$ MEFs, and these accumulated efficiently in mAgo2 (Fig. 5a). For comparison, we generated a *tRNA-mir-155* fusion that includes the endogenous Dicer-substrate *pre-mir-155* hairpin. Northern blotting of mAgo2 immunoprecipitates from *Dicer*$^{-/-}$ MEFs transfected with these constructs showed they contain *pre-mir-155* hairpin, but not mature miR-155 (Fig. 5a).

Northern blotting does not directly demonstrate that the detected small RNAs constitute a substantial fraction of total small RNAs in these cells. We therefore performed end labeling of total RNAs from mAgo2 immunoprecipitates. Strikingly, we observed that cells transfected with *tRNA-mir-451* accumulated specific RNAs in the <30nt range corresponding to matured miR-451 species (Fig. 5b). On the other hand, cells transfected with *tRNA-mir-155* accumulated a ~60 nt band at a level higher than control *Dicer*$^{-/-}$ MEFs or ones expressing *tRNA-mir-451* (Fig. 5b); we infer this to correspond to *pre-mir-155*. Therefore these tRNA constructs generate sufficient levels of small RNAs to impact the total small RNA pool in *Dicer*$^{-/-}$ cells.

With these validations in hand, we compared their effects on mAgo2 levels. Transfection of *tRNA-mir-451* substantially rescued instability of mAgo2 in *Dicer*$^{-/-}$ cells following CHX treatment (Fig. 5c). In contrast, *tRNA-mir-155* provided only slight improvement of mAgo2 stability compared to empty *tRNA-lys* vector alone (Fig. 5c). Immunoprecipitation experiments confirmed the reduction of mAgo2 under these conditions (Supplementary Fig.

4c). Therefore, while a population of pre-miRNA hairpins have the capacity to associate with mAgo2 in the absence of Dicer (Fig. 5a, b), these are not competent to protect mAgo2 from turnover.

To provide further evidence for this, we generated a *tRNA-mir-451* cleavage mutant (CM) bearing centrally bulged sites, a configuration that is competent for Ago loading but incompetent for mAgo2 cleavage[29]. We confirmed that *tRNA-mir-451CM* loads into mAgo2 in *Dicer*$^{-/-}$ cells but remains arrested as a *pre-mir-451* hairpin (Fig. 5d). We observed that *tRNA-mir-451-CM* was unable to stabilize mAgo2 (Fig. 5e), providing further evidence that mere RNA association may not suffice for mAgo2 stability. We hypothesize that the conformation of pre-miRNA-loaded Ago differs from the mature single-stranded complex, and that only the latter is fully licensed for stability *in vivo*.

Rescue of *Drosophila* AGO1 by synthetic miRNAs but not siRNAs

Finally, we returned to the *Drosophila* system to ask whether the reintroduction of small RNAs could rescue the instability of AGO1 in cells with impaired miRNA biogenesis. As Dicer-independent miRNAs have not yet been identified in this species, we turned to synthetic small RNA duplexes. This experimental strategy has the advantage of using the *Drosophila*-specific feature of Argonaute sorting to potentially distinguish the impact of siRNA loading from miRNA loading on AGO1 stability.

We earlier used synthetic miR-276a duplexes to dissect the mechanism of AGO1 loading in vitro[34]. Here, we evaluated the capacity of synthetic wild-type miR-276a duplex to repress target sensors when transfected into S2 cells. Both mature and star species of *mir-276a* are competent for target regulation of cognate luciferase sensors, when expressed as pri-miRNA transcripts from transfected plasmids[35] (Fig. 5f). However, we obtained much stronger repression of these sensors in S2 cells transfected with the synthetic miR-276a duplex, indicating that it efficiently populates functional Argonaute complexes. We utilized S2 cells that were doubly treated with *GFP*, *drosha*, *pasha*, or *dicer-1* dsRNA, and further introduced either synthetic fully-paired siRNA duplex (used in mammalian cell tests in Fig. 4f) or miR-276a duplex. We observed a mild improvement of AGO1 stability in the absence of miRNA biogenesis with the siRNA duplex, but observed robust recovery of AGO1 accumulation in the presence of synthetic miR-276a duplex (Fig. 5g). These tests specifically demonstrate that sorting of small RNAs to AGO1 are indeed required to maintain AGO1 stability.

Discussion

Model figures of small RNA biogenesis pathways often provide the impression that these processes are constitutive, inflexible and inexorable. However, diverse mechanisms that regulate small RNA biogenesis and function have been uncovered recently[5]. Notably, many of these mechanisms provide homeostatic control over the levels of small RNA biogenesis factors and/or their resultant small RNAs. The revised picture is that small RNA biogenesis and function are subject to constant tuning to maintain appropriate levels of the factors involved, and to provide systems that permit reversibility or enhancement of small RNA functions. In this sense, our knowledge of small RNA pathways has now come to par with

other signaling pathways and regulatory networks, which are almost universally subject to multilayer regulation.

In this study, we used both *Drosophila* and mammalian systems to demonstrate sensitive mechanisms that normalize levels of miRNA biogenesis to the abundance of Argonaute effector proteins. Recent structural studies of full-length mammalian Argonaute provide a framework for rationalizing the turnover of unloaded Argonautes, including the observation that Ago2 adopts a protease-resistant tight structure upon complexing with a small RNA[36,37]. This perspective is complemented by studies using Hsp90 inhibitors, which demonstrate conformational changes are required to load Argonautes with small RNAs leading to a stable state[9–13].

While this work was under revision, Gregory and colleagues reported that loss of miRNA biogenesis in ES cells (bearing *DGCR8* or *Dicer* mutations) similarly results in post-transcriptional loss of mAgo2 protein[38]. Our work agrees with this, and broadens this concept across multiple species, including both germline and somatic cells. In addition, our studies not only highlight that loss of miRNA biogenesis destabilizes Argonaute proteins, but that an excess of Argonaute proteins are normally made and can be stabilized by increasing miRNA transcription. We demonstrated this by clonal analysis of single-copy inducible miRNA transgenes, within the intact animal, and showed that activating the transcription of various miRNA loci was sufficient to elevate AGO1 protein levels (Fig. 3).

Such a homeostatic response was not expected, given that elevation of Argonaute proteins can increase the abundance of siRNAs[39] or miRNAs[40,41] and that quantitative measurements indicated an excess of miRNA species over Argonaute proteins[42], at least in certain systems. We note that the effects of elevated Argonaute proteins has mostly been studied with respect to co-transfected miRNA constructs and siRNAs; thus, influence of this manipulation on endogenous miRNA pools remain to be understood. In addition, miRNA:Argonaute stoichiometry was examined in cancer cells[42], and remains to be studied in tissues, or at least primary cells[43]. We believe that it makes physiological sense for there to be excess Argonaute proteins relative to miRNAs, since if Argonautes were limiting, then mere tissue-specific changes in the overall transcription of miRNA loci might result in substantial competition for Argonaute occupancy. This would not rule out that the transcription of Argonaute genes might itself be regulated to help normalize their protein levels with overall tissue-specific changes in bulk miRNA transcription; perhaps both strategies work in concert.

Interestingly, we find that the *Drosophila* RNAi effector AGO2 is not sensitive to the status of siRNA biogenesis. Why might homeostatic mechanisms exist specifically for miRNA effector Argonautes? One possibility is to prevent the misloading of unintended small RNAs into miRISCs, since this regulatory complex has capacity to regulate off-targets bearing minimal sequence complementarity. We showed that the RNAi pathway actively prevents loading of endo-siRNAs into AGO1[27], and a trimming and tailing mechanism further culls siRNAs loaded into miRISCs based on their atypically extensive target pairing[44]. The destabilization of unloaded miRNA effectors may be another mechanism to ensure purity of this Argonaute pool. On the other hand, the rarity of extensively-paired "siRNA-type"

targets may mean that misloading of AGO2 is better tolerated, and perhaps a pool of unloaded AGO2 may ensure a timely response to viral infections by allowing large amounts of siRISC to be generated quickly.

The ubiquitin-proteasome system contributes to Argonaute homeostasis, extending a theme from other recent studies that demonstrate temporal or cell state-specific ubiquitination and degradation of Argonaute and Piwi proteins[45,46]. In support of this notion, we utilize not only chemical inhibitors, but also genuine genetic manipulations of the proteasome. We showed that *Drosophila* AGO1 is increased in cells depleted of *uba1* (the sole *Drosophila* ubiquitin activating enzyme) or that express a dominant-negative proteasome subunit (DTS5), indicating that excess miRNA Argonaute effectors are being turned over in vivo. Recently, autophagy was reported to degrade Ago2 in HeLa cells[31] and in *DGCR8*$^{-/-}$ ES cells[38]. The latter work is consistent with conclusions regarding instability of Argonautes in the absence of miRNA biogenesis. On the other hand, we did not observe substantial effects of autophagy inhibition in either our *Drosophila* or mouse cell culture systems, even though we confirmed defective autophagy by accumulation of LC3-II (Supplementary Fig. 5). However, it is conceivable that both degradation pathways contribute to the observed phenomenon, with the relative contributions being determined by cell type and culture conditions.

Finally, our studies used novel non-canonical miRNA expression vectors to distinguish between the pre-miRNA-associated Argonaute state and the mature, functional miRISC state. In particular, our results indicate that Argonaute stability is not only sensitive to the overall availability of miRNAs, but also to its state as a mature complex (Fig. 5). Therefore, even though *Dicer*$^{-/-}$ cells accumulate pre-miRNAs, and these can associate with Argonaute proteins[47], RNA association alone does not seem sufficient for full stability. In combination with our data that *Drosophila* AGO1 can be stabilized by increasing miRNA transcription, we conclude that metazoan cells harbor sensitive mechanisms that actively harmonize the levels of miRNA effector Argonautes to the status of miRNA biogenesis.

Online Methods

Drosophila stocks, clonal analysis and immunostaining

Mutant alleles and transgenes described in this work include *AGO1[k08121]*[48], *AGO1[14]*[49], *dcr-1[Q1147X]*[28], *dcr-1[21B2]*[20], *dicer-1[30D2]*[20], *dicer-1[37A1]*[20], *dicer-1[38E3]*[20], *pasha[KO]*[50], *pasha[36B2]*[20], *drosha[21K11]*[8],*GW182-RNAi* (VDRC #103581), *shep-RNAi* (VDRC #37863), *hs-AGO1*[48], *UAS-DTS5*[51], *UAS-mir-124* and *UAS-mir-124-mutant*[52], and other *UAS-miRNA* transgenes recently described from a genome-wide collection[53]. *ptc-gal4*, and *uba1-RNAi* (TRiP line) were obtained from the Bloomington Stock Center.

Imaginal disc clones were induced 72 hours after egg deposition with either 75 minute (MARCM) or 15 minute (FLP-out) 37°C heatshock, and fixed 72 hours later. Tester stocks were:

2R MARCM stock: *y,w, hsFLP, UAS-CD8GFP ; FRT42D, tub-gal80 ; tub-gal4 / TM6B*

3R MARCM stock: *y,w, hsFLP, UAS-CD8GFP ; ; tub-gal4, FRT82B, tub-gal80 / TM6B*

FLP-out clone stock: *y,w, hsFLP ; ; act>CD2>gal4, UASGFPnls*

FLP-out stock: *hsFLP, UASGFPnls ; + / SM5-TM6 / tub>gal80>gal4*

Immunostaining was performed as previously described[54]. Ovarian follicle cell clones were induced with 15 minute heatshock of young mated female adults and fixed 72 hours later[20]. Antibodies used were Chicken anti-GFP (1/1000, Abcam), Rabbit anti-Mei-P26 (1/1000)[55], mouse anti-Ago1 1B8 (1/1000) (gift from Haruhiko Siomi), Rabbit anti-GW182 (1/500) (this study), Rabbit anti-Gal4 DBD (1/150, Santa Cruz sc-577).

To genotype the *dcr-2* alleles, the following allele-specific PCR primers were used: dcr2[L811X] test F_CAGTCAACAAGGCCGATAAGAGC and dcr2 [L811] wt ASO R_ACAAAGAACGGATGCCAAATCTTC for the wildtype *dcr-2* allele; dcr2 [L811X] ASO_ATGGTATTCCGCGATATCTTTGG and dcr2[L811X] test R_CACCTTTGTGACCAGCATGGG for the *dcr-2[L811fsx]* allele.

Drosophila S2 cell studies

We depleted small RNA factors from S2R+ cells by soaking with double stranded RNA as described[56], using previously validated templates[24]. All soaking experiments are the result of 2 rounds of RNAi soaking for 4 days each. 4 days after the first dsRNA soaking, total cell number was re-normalized before performing the second round of soaking. For S2 cell western blots, we used Rabbit anti-AGO1 (1/1000, Abcam ab5070) and mouse anti-alpha Tubulin (1/1000). To quantify proteins, signals generated by the ECL reagent were captured by Fujifilm LAS-3000 Imager using non-saturating exposures. Intensity of individual bands on the blots was measured by ImageGauge under the "Quant" mode. α-tubulin was used as loading control to normalize the amount of individual samples.

For qRT-PCR analysis of *AGO1* transcript levels, we used these primer sets: AGO1-2678+ (5'-TGTGGGACGACAATCACTTT-3'), AGO1-2807- (5'-CAGATGATATCTGGCACGGA-3'), AGO1-1015+ (5'-GTCATTGACTTCATGTGCGA-3'), AGO1-1195- (5'-AGTGGGAATGATTGCATCTG-3'). For miRNA and siRNA transfection experiments, 100 pmole of 5' phosphorylated miR-276a/star duplex or scrambled siRNA were transfected into S2 cells, 7 days after dsRNA soaking. The RNA was harvested 24 hours after transfection. For luciferase assays, a psiCHECK plasmid bearing two perfect sites for miR-276a downstream of a Renilla luciferase gene (25ng per well) were co-transfected with ub-Gal4 (12.5ng/well) and either pUAS-DsRed-mir-276a (25ng/well) or miR-276a duplex (15.6pmole per well) for 72 h in 96-well plates. Luciferase activities were measured with the Dual-Glo Luciferase Assay System (Promega).

Mammalian plasmids and siRNAs

Dicer-expressing plasmid (pCK-FLAG-Dicer) was a gift of Dr. V. Narry Kim (Seoul National University, Korea). The scrambled siRNA control was purchased from IDT. The miRNA-expressing and control constructs (tRNA[lys], tRNA-mir-451, tRNA-mir-451cm,

and tRNA-mir-155) were cloned into pCR2.1-TOPO vector (Life Technologies) as previously described[33]. Oligo sequences for miRNA cloning were:

tRNAlys3_F GcccggatagctcagtcggtagagcaTcagactttTaatctgagggtccagggtTcaagtccctg

tRNAlys3_R gaggaaaaaaaagatacCGCCCGAAcagggacttgAaccc

tRNAlys3_451wt_R
AAAAACCATTACCATTACTAAACTCAGTAATGGTAACGGTTTCGCCCGAACAGGGACTTGAACCC

tRNAlys3_451cm_R
AAAAACCATTAaaATTACTAAACTCAGTAATGGTAACGGTTTCGCCCGAACAGGGACTTGAACCC

tRNAlys3_mir155_R
AAAAATGTTAATGCTAATATGTAGGAGTCAGTTGGAGGCAAAAACCCCTATCACGATTAGCATTAACGCCCGAACAGGGACTTGAACCC

Mammalian cell studies

Dicer$^{-/-}$ mouse embryonic fibroblasts (MEFs) and human 293T cells were maintained in DMEM, high glucose, GlutaMAX with 10% heat-inactivated FBS (Sigma) and 1% Penicillin-Streptomycin (Life Technologies) and incubated in a humidified 37°C/5% CO2 incubator. Lipofectamine 2000 (Life Technologies) was used to transfect cells according to the manufacturer's manual. To study mAgo2 stability, 50 μg/ml cycloheximide (CHX, Calbiochem) was added to *Dicer*$^{-/-}$ MEFs 24 h after transfection. The cells were harvested at 5 h and 10–12 h after CHX addition. To inhibit proteasome activity, cells were treated with both CHX (25 μg/ml) and MG132 (25 μM) or DMSO for 5 and 10 h. To inhibit autophagy pathway activity, cells were co-treated with CHX (25 μg/ml) and DMSO or Bafilomycin A1 (100 nM) for 4 and 8 h. Total proteins were obtained by lysing the cells with IP/Extract buffer (20mM Tris-HCl pH 7.5, 150mM NaCl, 2mM $MgCl_2$, 5% Glycerol, 5% NP-40, 2mM DTT). The following antibodies were used in Western blotting: anti-mAgo2 (MA2, 1:5000; a kind gift from Dr. Donal O'Carroll, EMBL); anti-α-tubulin (1:1000); anti-HA (F-7, 1:000, Santa Cruz Biotechnology, Inc). Western signals were quantified as described above.

Total RNA was extracted by Trizol reagent (Life Technologies), and the resulting RNA was subjected to qRT-PCR analysis and Northern blotting. We performed three replicate qRT-PCR assays with the following primer sets: qmmu-Ago2_F (5′-AGTTCCAGCAGGTTCTCCAC-3′), qmmu-Ago2_R (5′-ATGTTCCCACTCTTCCCAAC-3′), qmmu-GAPDH_F (5′-TGTGTCCGTCGTGGATCTGA-3′), qmmu-GAPDH_R (5′-CCTGCTTCACCACCTTCTTGA-3′). For Northern blotting, RNA samples were separated on 20% urea polyacrylamide denaturing gels (National Diagnostics), transferred to GeneScreen Plus (Perkin Elmer), and probed with γ-^{32}P-labeled DNA oligonucleotides antisense to the miRNAs of interest at 45°C overnight. The membranes were washed with 2X SSC/0.1% SDS at 45°C for 4 times for 15 min each, then exposed to an imaging plate (Fujifilm). The sequences of probes used in our studies are: miR-155 (5′-

ACCCCTATCACGATTAGCATTAA-3′), miR-451 (5′-AACTCAGTAATGGTAACGGTTT-3′), let-7 (5′-ACTATACAACCTACTACCTCA-3′).

To analyze mAgo2-associated RNA, cell lysates were cleared and then incubated with mouse mAgo2 antibody (2D4, Wako)-conjugated Dynabeads Protein G (Invitrogen). The mAgo2-associated RNA was extracted with phenol/chloroform/isoamyl alcohol (25:24:1), followed by ethanol precipitation at −20°C overnight. The RNA was resuspended in 15μl water, divided into half, and subjected to Northern blotting or a total labeling experiment. To label total RNA associated to mAgo2, RNA samples were first 5' dephosphorylated with antarctic phosphatase (NEB) in the presence of 20 units of RNaseOUT (Life Technology) at 37°C for 1 h. The antarctic phosphatase was inactivated at 70°C for 10 min. The resulting RNA samples were then 5' phosphorylated with γ-^{32}P-ATP by PNK (NEB) in the presence of 20 units of RNaseOUT at 37°C for 1 h. The unincorporated γ-^{32}P-ATP was removed by Illustra MicroSpin G-25 Columns (GE Healthcare Life Sciences), and half of the samples were loaded onto 20% urea polyacrylamide denaturing gels with 2× Gel Loading Buffer II (Ambion). The signals were exposed to an imaging plate for 10 min.

Supplementary Material

Refer to Web version on PubMed Central for supplementary material.

Acknowledgments

We thank G. Meister (Universität Regensburg, Regensburg, Germany), M. Overholtzer (Sloan-Kettering Institute, New York, NY USA), X. Jiang (Sloan-Kettering Institute, New York, NY USA), K. Okamura (Temasek Institute) V. Kim (Seoul National University, Seoul Korea), H. Siomi (Keio University, Tokyo Japan), A. Tarakhovsky (Rockefeller University, New York, NY USA), D. O'Carroll (EMBL, Monterotondo Scalo Italy), R. Carthew (Northwestern University, Chicago USA), F. Schweisguth (Institut Pasteur, Paris, France), F. Gao (University of Massachusetts Medical School, Worcester, MA USA), the Vienna Drosophila RNAi Center (Vienna, Austria) and the Bloomington Drosophila Stock Center (Bloomington, IN USA) for reagents and discussions. Work in J.L.'s group was supported by UK Medical Research Council. G.A was supported by the Malaysian Ministry of Higher Education. Work in E.L.'s group was supported by the US National Institutes of Health R01-GM083300.

References

1. Czech B, Hannon GJ. Small RNA sorting: matchmaking for Argonautes. Nat Rev Genet. 2010; 12:19–31. [PubMed: 21116305]
2. Kim VN, Han J, Siomi MC. Biogenesis of small RNAs in animals. Nat Rev Mol Cell Biol. 2009; 10:126–139. [PubMed: 19165215]
3. Yang JS, Lai EC. Alternative miRNA biogenesis pathways and the interpretation of core miRNA pathway mutants. Mol Cell. 2011; 43:892–903. [PubMed: 21925378]
4. Fabian MR, Sonenberg N. The mechanics of miRNA-mediated gene silencing: a look under the hood of miRISC. Nat Struct Mol Biol. 2012; 19:586–593. [PubMed: 22664986]
5. Heo I, Kim VN. Regulating the regulators: posttranslational modifications of RNA silencing factors. Cell. 2009; 139:28–31. [PubMed: 19804751]
6. Han J, et al. Posttranscriptional crossregulation between Drosha and DGCR8. Cell. 2009; 136:75–84. [PubMed: 19135890]
7. Kadener S, et al. Genome-wide identification of targets of the drosha-pasha/DGCR8 complex. RNA. 2009; 15:537–545. [PubMed: 19223442]
8. Smibert P, et al. A Drosophila genetic screen yields allelic series of core microRNA biogenesis factors and reveals post-developmental roles for microRNAs. RNA. 2011; 17:1997–2010. [PubMed: 21947201]

9. Iki T, Yoshikawa M, Meshi T, Ishikawa M. Cyclophilin 40 facilitates HSP90-mediated RISC assembly in plants. Embo J. 2012; 31:267–278. [PubMed: 22045333]
10. Iki T, et al. In vitro assembly of plant RNA-induced silencing complexes facilitated by molecular chaperone HSP90. Mol Cell. 2010; 39:282–291. [PubMed: 20605502]
11. Miyoshi T, Takeuchi A, Siomi H, Siomi MC. A direct role for Hsp90 in pre-RISC formation in Drosophila. Nat Struct Mol Biol. 2011; 18:516.
12. Iwasaki S, et al. Hsc70/Hsp90 chaperone machinery mediates ATP-dependent RISC loading of small RNA duplexes. Mol Cell. 2010; 39:292–299. [PubMed: 20605501]
13. Johnston M, Geoffroy MC, Sobala A, Hay R, Hutvagner G. HSP90 protein stabilizes unloaded argonaute complexes and microscopic P-bodies in human cells. Mol Biol Cell. 2010; 21:1462–1469. [PubMed: 20237157]
14. Ishizu H, Siomi H, Siomi MC. Biology of PIWI-interacting RNAs: new insights into biogenesis and function inside and outside of germlines. Genes Dev. 2012; 26:2361–2373. [PubMed: 23124062]
15. Handler D, et al. A systematic analysis of Drosophila TUDOR domain-containing proteins identifies Vreteno and the Tdrd12 family as essential primary piRNA pathway factors. EMBO J. 2011; 30:3977–3993. [PubMed: 21863019]
16. Liu Q, et al. R2D2, a bridge between the initiation and effector steps of the Drosophila RNAi pathway. Science. 2003; 301:1921–1925. [PubMed: 14512631]
17. Jiang F, et al. Dicer-1 and R3D1-L catalyze microRNA maturation in Drosophila. Genes Dev. 2005; 19:1674–1679. [PubMed: 15985611]
18. Forstemann K, Horwich MD, Wee L, Tomari Y, Zamore PD. Drosophila microRNAs are sorted into functionally distinct argonaute complexes after production by dicer-1. Cell. 2007; 130:287–297. [PubMed: 17662943]
19. Miyoshi K, Okada TN, Siomi H, Siomi MC. Characterization of the miRNA-RISC loading complex and miRNA-RISC formed in the Drosophila miRNA pathway. RNA. 2009; 15:1282–1291. [PubMed: 19451544]
20. Azzam G, Smibert P, Lai EC, Liu JL. Drosophila Argonaute 1 and its miRNA biogenesis partners are required for oocyte formation and germline cell division. Dev Biol. 2012
21. Herranz H, et al. The miRNA machinery targets Mei-P26 and regulates Myc protein levels in the Drosophila wing. EMBO J. 2010; 29:1688–1698. [PubMed: 20400939]
22. Yao B, La LB, Chen YC, Chang LJ, Chan EK. Defining a new role of GW182 in maintaining miRNA stability. EMBO Rep. 2012; 13:1102–1108. [PubMed: 23090477]
23. Neumuller RA, et al. Mei-P26 regulates microRNAs and cell growth in the Drosophila ovarian stem cell lineage. Nature. 2008
24. Okamura K, et al. The Drosophila hairpin RNA pathway generates endogenous short interfering RNAs. Nature. 2008; 453:803–806. [PubMed: 18463630]
25. Czech B, et al. Hierarchical rules for Argonaute loading in Drosophila. Mol Cell. 2009; 36:445–456. [PubMed: 19917252]
26. Czech B, et al. An endogenous siRNA pathway in Drosophila. Nature. 2008; 453:798–802. [PubMed: 18463631]
27. Okamura K, Robine N, Liu Y, Liu Q, Lai EC. R2D2 organizes small regulatory RNA pathways in Drosophila. Mol Cell Biol. 2011; 31:884–896. [PubMed: 21135122]
28. Lee YS, et al. Distinct Roles for Drosophila Dicer-1 and Dicer-2 in the siRNA/miRNA Silencing Pathways. Cell. 2004; 117:69–81. [PubMed: 15066283]
29. Yang JS, et al. Conserved vertebrate mir-451 provides a platform for Dicer-independent, Ago2-mediated microRNA biogenesis. Proc Natl Acad Sci U S A. 2010; 107:15163–15168. [PubMed: 20699384]
30. Castilla-Llorente V, et al. Mammalian GW220/TNGW1 is essential for the formation of GW/P bodies containing miRISC. J Cell Biol. 2012; 198:529–544. [PubMed: 22891262]
31. Gibbings D, et al. Selective autophagy degrades DICER and AGO2 and regulates miRNA activity. Nat Cell Biol. 2012; 14:1314–1321. [PubMed: 23143396]

32. Yang JS, Lai EC. Dicer-independent, Ago2-mediated microRNA biogenesis in vertebrates. Cell Cycle. 2010; 9:4455–4460. [PubMed: 21088485]
33. Maurin T, Cazalla D, Yang JS, Bortolamiol-Becet D, Lai EC. RNase III-independent microRNA biogenesis in mammalian cells. RNA. 2012; 18:2166–2173. [PubMed: 23097423]
34. Okamura K, Liu N, Lai EC. Distinct mechanisms for microRNA strand selection by Drosophila Argonautes. Mol Cell. 2009; 36:431–444. [PubMed: 19917251]
35. Okamura K, et al. The regulatory activity of microRNA* species has substantial influence on microRNA and 3' UTR evolution. Nat Struct Mol Biol. 2008; 15:354–363. [PubMed: 18376413]
36. Elkayam E, et al. The Structure of Human Argonaute-2 in Complex with miR-20a. Cell. 2012; 150:100–110. [PubMed: 22682761]
37. Schirle NT, MacRae IJ. The crystal structure of human Argonaute2. Science. 2012; 336:1037–1040. [PubMed: 22539551]
38. Martinez NJ, Gregory RI. Argonaute2 expression is post-transcriptionally coupled to microRNA abundance. Rna. 2013; 19:605–612. [PubMed: 23485552]
39. Yigit E, et al. Analysis of the C. elegans Argonaute family reveals that distinct Argonautes act sequentially during RNAi. Cell. 2006; 127:747–757. [PubMed: 17110334]
40. Diederichs S, Haber DA. Dual Role for Argonautes in MicroRNA Processing and Posttranscriptional Regulation of MicroRNA Expression. Cell. 2007; 131:1097–1108. [PubMed: 18083100]
41. Yang JS, Maurin T, Lai EC. Functional parameters of Dicer-independent microRNA biogenesis. RNA. 2012; 18:945–957. [PubMed: 22461413]
42. Janas MM, et al. Alternative RISC assembly: binding and repression of microRNA-mRNA duplexes by human Ago proteins. RNA. 2012; 18:2041–2055. [PubMed: 23019594]
43. Wang D, et al. Quantitative functions of Argonaute proteins in mammalian development. Genes Dev. 2012; 26:693–704. [PubMed: 22474261]
44. Ameres SL, Hung JH, Xu J, Weng Z, Zamore PD. Target RNA-directed tailing and trimming purifies the sorting of endo-siRNAs between the two Drosophila Argonaute proteins. RNA. 2011; 17:54–63. [PubMed: 21106652]
45. Zhao S, et al. piRNA-Triggered MIWI Ubiquitination and Removal by APC/C in Late Spermatogenesis. Dev Cell. 2013; 24:13–25. [PubMed: 23328397]
46. Bronevetsky Y, et al. T cell activation induces proteasomal degradation of Argonaute and rapid remodeling of the microRNA repertoire. J Exp Med. 2013; 210:417–432. [PubMed: 23382546]
47. Tan GS, et al. Expanded RNA-binding activities of mammalian Argonaute 2. Nucleic Acids Res. 2009; 37:7533–7545. [PubMed: 19808937]

Supplementary References

48. Kataoka Y, Takeichi M, Uemura T. Developmental roles and molecular characterization of a Drosophila homologue of Arabidopsis Argonaute1, the founder of a novel gene superfamily. Genes Cells. 2001; 6:313–325. [PubMed: 11318874]
49. Yang L, et al. Argonaute 1 regulates the fate of germline stem cells in Drosophila. Development. 2007; 134:4265–4272. [PubMed: 17993467]
50. Martin R, et al. A Drosophila pasha mutant distinguishes the canonical miRNA and mirtron pathways. Mol Cell Biol. 2009; 29:861–870. [PubMed: 19047376]
51. Schweisguth F. Dominant-negative mutation in the b2 and b6 proteasome-subunit genes affect alternative cell fate decisions in the *Drosophila* sense organ lineage. Proc. Natl. Acad. Sci. USA. 1999; 96:11382–11386. [PubMed: 10500185]
52. Xu XL, Li Y, Wang F, Gao FB. The steady-state level of the nervous-system-specific microRNA-124a is regulated by dFMR1 in Drosophila. J Neurosci. 2008; 28:11883–11889. [PubMed: 19005053]
53. Bejarano F, et al. A genome-wide transgenic resource for conditional expression of Drosophila microRNAs. Development. 2012; 139:2821–2831. [PubMed: 22745315]

54. Lai EC, Rubin GM. *neuralized* functions cell-autonomously to regulate a subset of Notch-dependent processes during adult *Drosophila* development. Dev Biol. 2001; 231:217–233. [PubMed: 11180964]

55. Liu N, Han H, Lasko P. Vasa promotes Drosophila germline stem cell differentiation by activating mei-P26 translation by directly interacting with a (U)-rich motif in its 3' UTR. Genes Dev. 2009; 23:2742–2752. [PubMed: 19952109]

56. Okamura K, Hagen JW, Duan H, Tyler DM, Lai EC. The mirtron pathway generates microRNA-class regulatory RNAs in Drosophila. Cell. 2007; 130:89–100. [PubMed: 17599402]

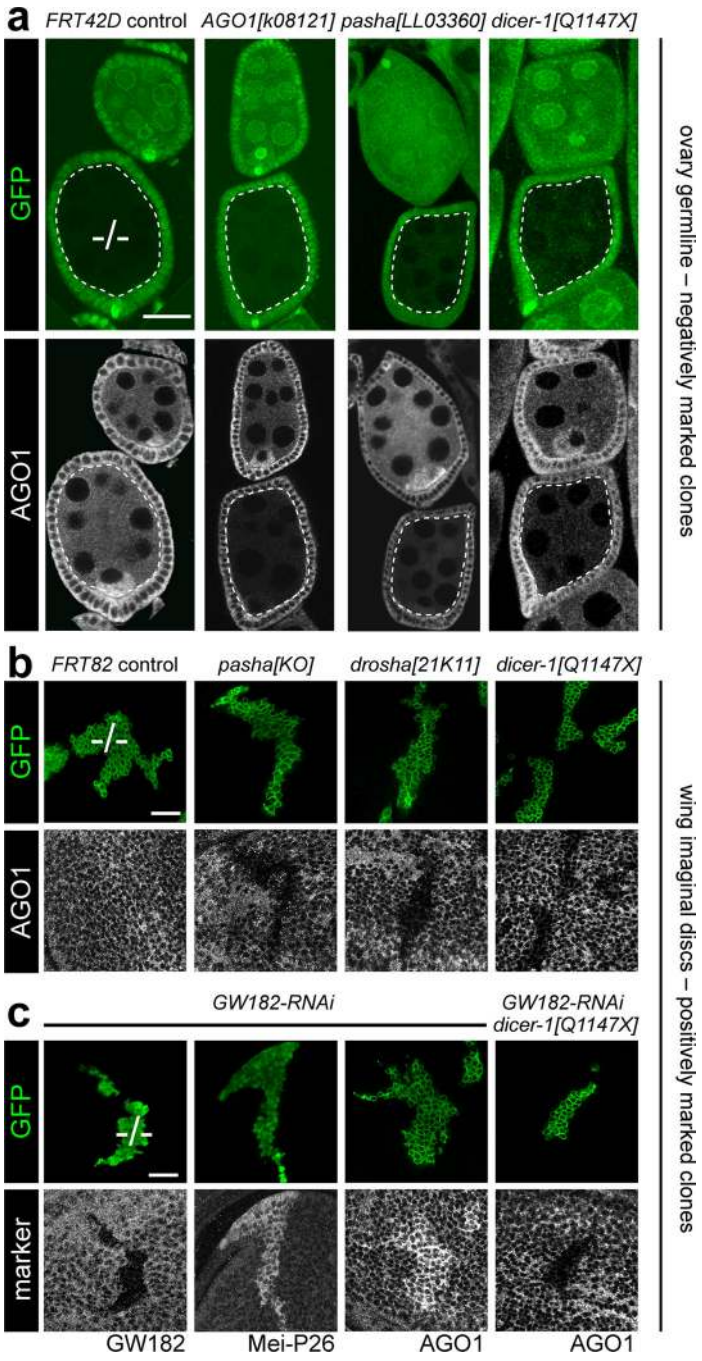

Figure 1. *Drosophila* AGO1 protein is reduced in the absence of miRNA biogenesis and accumulates upon depletion of GW182

(a) Ovarioles bearing negatively-marked mutant clones (lacking GFP in green channel) stained for AGO1 protein (grayscale channel); scale bar = 20μm. Each genotype shows a pair of egg chambers, of which the bottom one contains a germline clone outlined in dotted lines ("−/−"). Control clone using the FRT42 chromosome shows the normal AGO1 pattern, whereas AGO1 is decreased in *AGO1*, *pasha* and *dicer-1* mutant germlines. (b) Positively-marked wing imaginal disc clones (expressing GFP, green channel) stained for AGO1

protein (grayscale channel); scale bar = 20μm. Control clone using the FRT82 chromosome shows no alteration of AGO1 levels, whereas null mutant clones of *pasha*, *drosha*, and *dicer-1* exhibit cell-autonomous reduction in AGO1 protein. (c) Epistasis analysis of *dicer-1* and *GW182*. Positively-marked wing disc clones were stained for various markers (grayscale channel) as labeled; scale bar = 20μm. Clones expressing RNAi against *GW182* exhibit reduced GW182 protein, de-repress the endogenous miRNA target Mei-P26, and accumulate AGO1. However, mutant clones of *dicer-1* that express *GW182*-RNAi display reduced AGO1 protein. See also Figs. S1–S3.

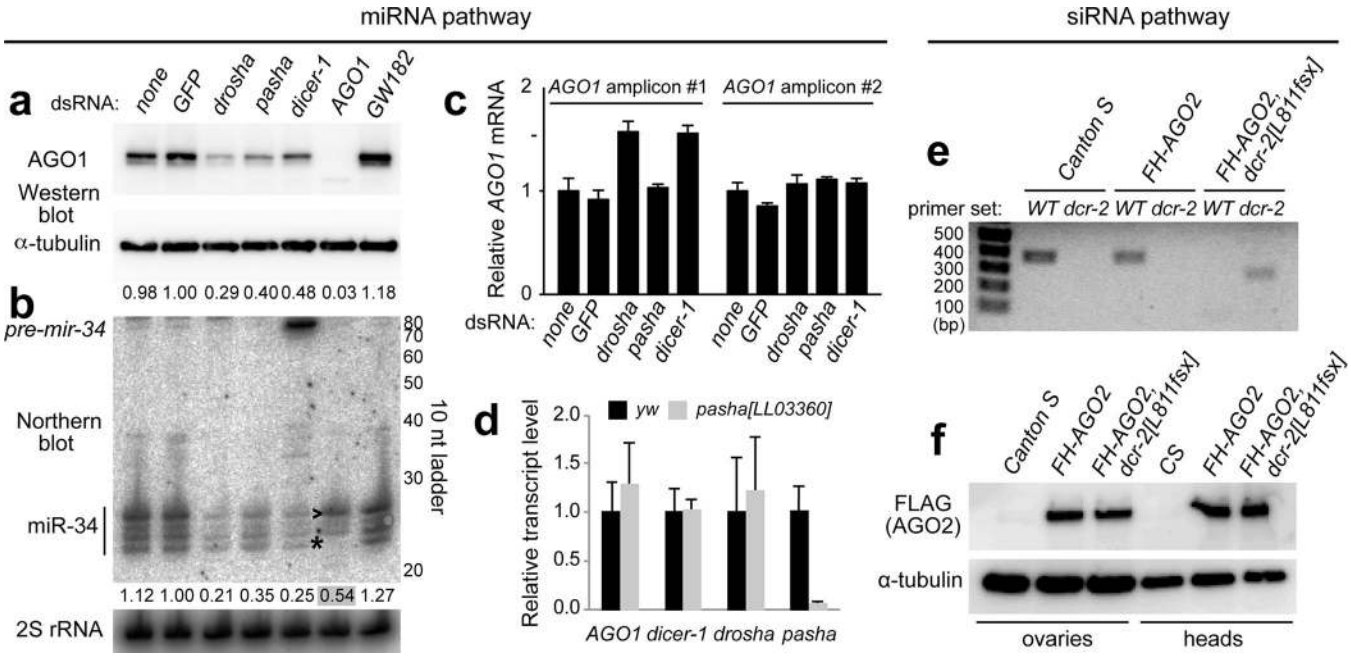

Figure 2. miRNA biogenesis stabilizes AGO1 post-transcriptionally, but siRNA biogenesis does not stabilize AGO2 in *Drosophila*

(a) Western analysis following knockdowns of miRNA factors in S2 cells recapitulated the AGO1 accumulation phenotypes of mutant disc clones. AGO1 protein was reduced following depletion of miRNA biogenesis factors *drosha*, *pasha* and *dicer-1*, and increased following knockdown of *GW182*. (b) Northern analysis of the same conditions shows parallel effects on miR-34. Depletion of miRNA biogenesis factors decreased mature miR-34 (and loss of *dicer-1* results in *pre-mir-34* accumulation), while knockdown of GW182 increased mature miR-34. Note that while loss of AGO1 protein is nearly complete upon *AGO1* knockdown, substantial miR-34 remains. This is likely due its re-sorting to AGO2, as evidenced by its altered length distribution (asterisk, *) and preferential accumulation of the largest isoform. (c) Assays of independent qPCR amplicons for *AGO1* reveal no substantial, reproducible, changes upon depletion of miRNA biogenesis factors in S2 cells (i.e., the mild increase of *AGO1* detected in some knockdowns using amplicon 1 were not verified by amplicon 2). Tests were done in triplicate for each sample. Error bars represent standard error of the mean. (d) qPCR analysis of miRNA pathway factors in *pasha* mutant third instar larvae showed no significant differences compared to *yellow white* (*yw*) control larvae, except for loss of *pasha* transcript. (e) Genotyping of *dcr-2*$^{+}$ (wildtype, WT) and *dcr-2[L811fsx]* using allele-specific primer pairs confirms the status of wildtype and *dcr-2* homozygous mutant backgrounds carrying *Flag-HA-AGO2* genomic transgenes. (F) Western blot analysis shows that AGO2 levels were unaffected by absence of Dcr-2. See also Fig. S6.

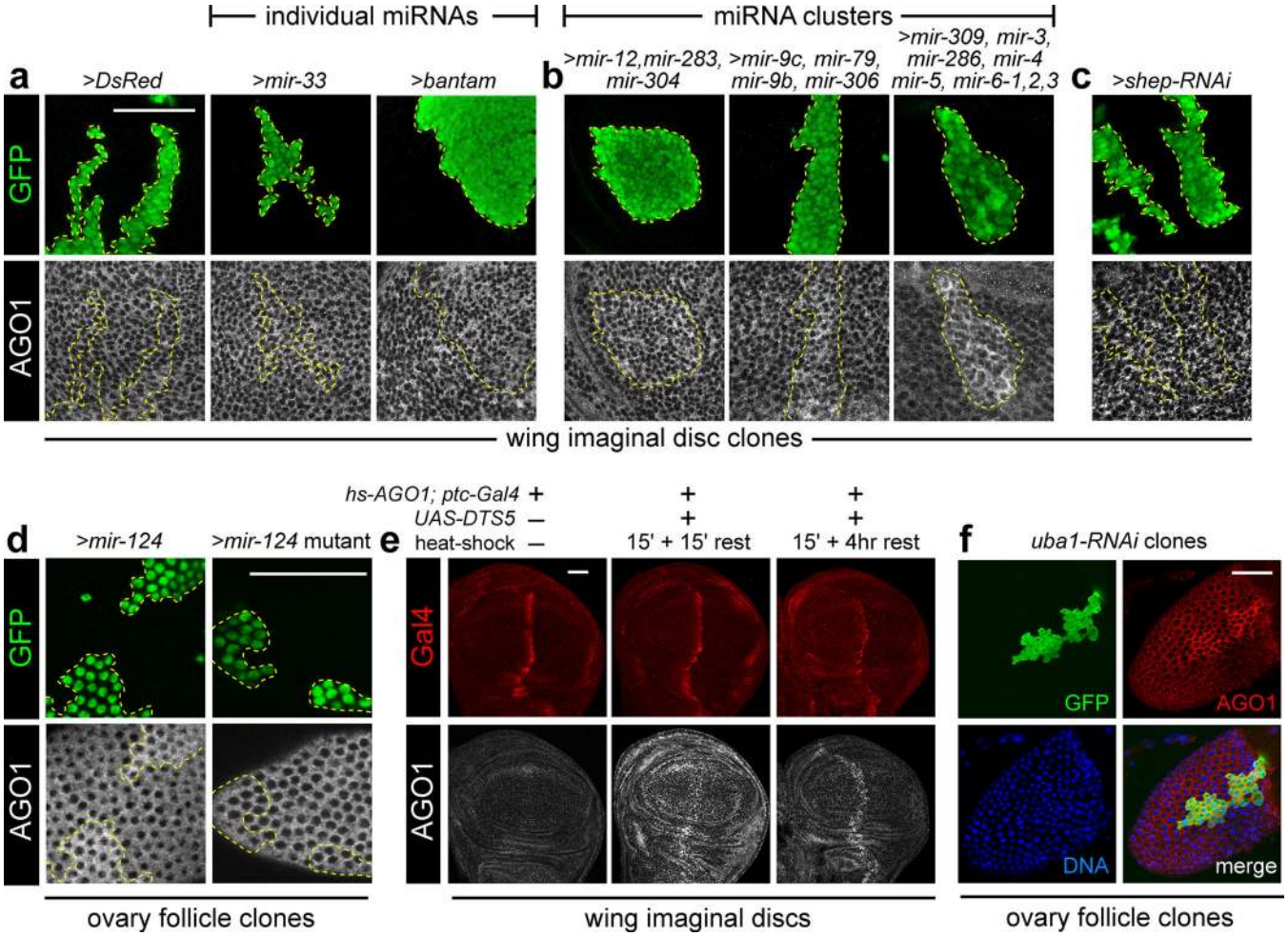

Figure 3. *Drosophila* AGO1 accumulates with increased miRNA transcription and is turned over by the ubiquitin-proteasome system

(a–c) FLP-out GFP-expressing clones (in green) expressing small RNA or protein constructs in wing imaginal discs. (a) Compared to control clones expressing DsRed, expression of individual miRNAs had marginal effects on AGO1 protein. (b) In contrast, expression of miRNA genomic clusters (containing 3, 4 or 8 miRNAs) all induced accumulation of AGO1. (c) Ectopic siRNAs, driven by expression of an inverted repeat RNAi trigger against *shep*, did not alter AGO1 levels. (d) AGO1 accumulation also occurs in ovarian follicle cells expressing wild-type *mir-124*, but not upon expression of processing-defective mutant *mir-124*. (e) Exogenous AGO1 is rapidly turned over by the proteasome. All discs contain *hs-AGO1* and *ptc-Gal4*; the middle and right discs also contained *UAS-DTS5*. Stainings for Gal4 (red channel) and AGO1 (gray scale) were processed in parallel and scanned using identical conditions. The larva from which the disc at left was dissected was not heat-shocked; a 15' heat-shock at 37°C followed by 15' recovery at 25°C before dissection generates ectopic AGO1 ubiquitously. Following a 4 hour recovery, ectopic AGO1 persisted only in the *ptc>DTS5* domain. (f) Inhibition of *Uba1* in follicle cells resulted in accumulation of endogenous AGO1. Scale bar for all images = 50μm.

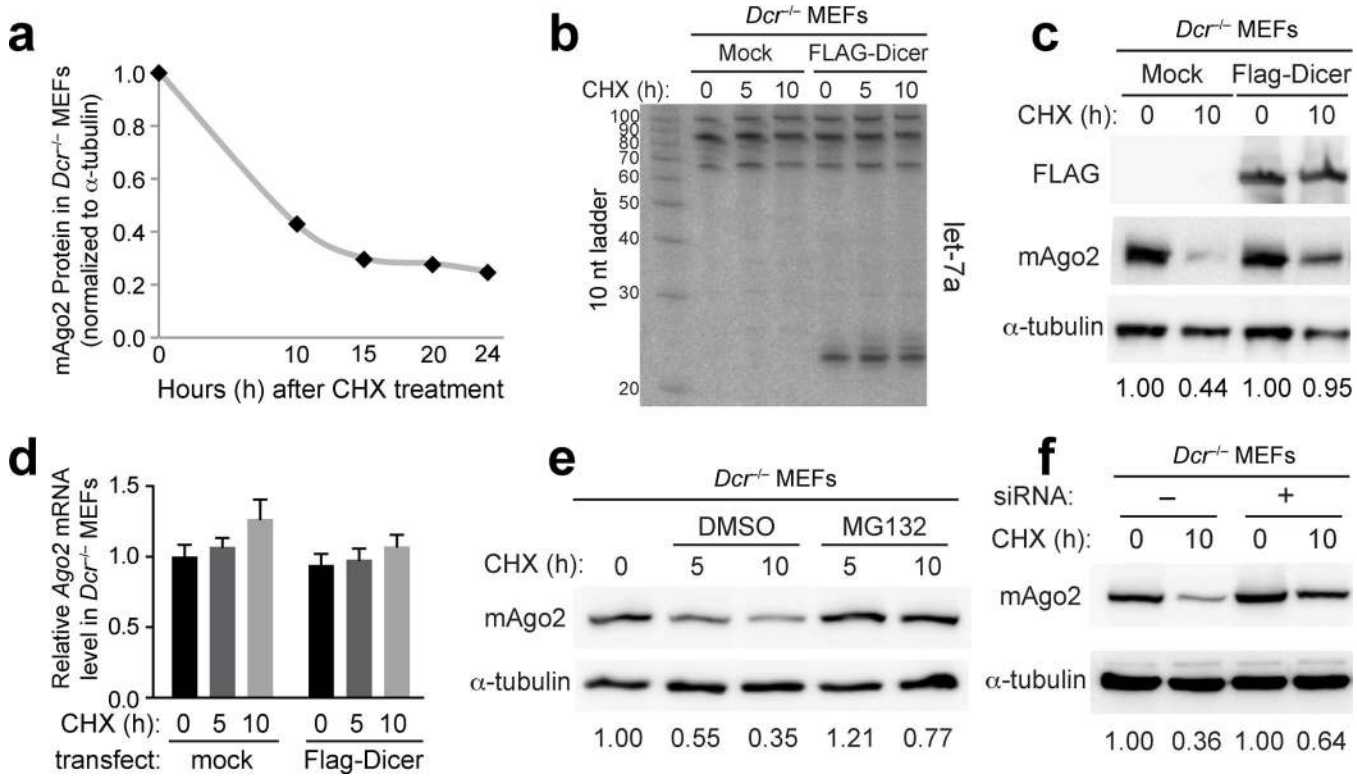

Figure 4. Mammalian Ago2 is stabilized by ongoing miRNA biogenesis. All experiments were performed in *Dicer*$^{-/-}$ cells, subjected to plasmid transfections and/or chemical treatments as noted

(a) *Dicer*$^{-/-}$ cells were treated with cycloheximide (CHX) for the indicated times, followed by Western blotting for endogenous mAgo2 and alpha-tubulin. The graph depicts instability of mAgo2 relative to alpha-tubulin. (b) Northern blot demonstrating that transfection of *Dicer*$^{-/-}$ cells with FLAG-Dicer plasmid rescued miRNA processing and accumulation of endogenous let-7a. (c) Western blot showing that mAgo2 exhibited increased accumulation in *Dicer*$^{-/-}$ cells following restoration of Dicer function. (d) qPCR analysis revealed no substantial change in *mAgo2* transcript levels following CHX treatment or restoration of Dicer. Tests were done in triplicate for each sample. Error bars represent standard error of the mean. (e) Western analysis of *Dicer*$^{-/-}$ MEFs cultured for 5 and 10 hours in the presence of CHX and vehicle control, or the proteasome inhibitor MG132. mAgo2 protein was degraded over time in DMSO-treated cells but this was partially stabilized by MG132. (f) Western blot demonstrating that transfection of generic siRNAs also improved the stability of mAgo2. See also Figs. S4–S6.

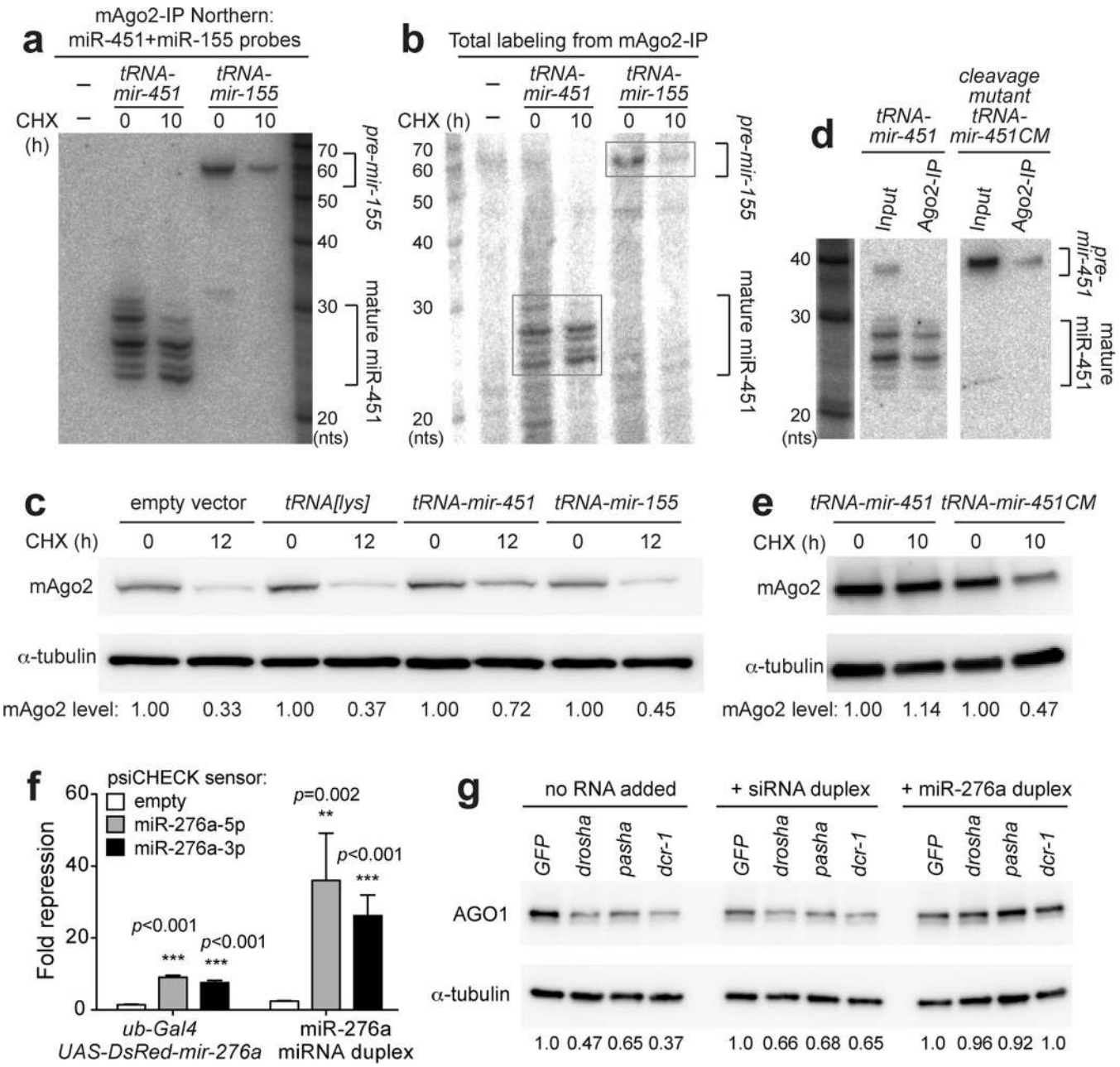

Figure 5. Accumulation of mouse and *Drosophila* Argonautes is dependent on loading with functional small RNAs

(a) *Dicer*$^{-/-}$ cells were transfected with *tRNA-mir-451* or *tRNA-mir-155* fusion constructs, and RNAs recovered from mAgo2-IP were subjected to Northern blotting. (b) RNA samples from (a) were subjected to 5'-end labelling to visualize all RNAs. Signals in mAgo2-IP derived mostly from mature miR-451 and *pre-mir-155*. (c) Western blot showing that mAgo2 was stabilized in cells expressing wild-type Dicer-independent *mir-451*, but not in cells expressing Dicer-dependent *mir-155* or *tRNA[lys]* parent construct. (d) A *tRNA-mir-451* cleavage mutant (CM) contains bulged nucleotides at its mAgo2 cleavage site. This arrests its processing as a pre-miRNA hairpin, as confirmed by Northern blotting of input

and mAgo2-IP material from transfected *Dicer*$^{-/-}$ cells. Note that cells expressing wild-type *tRNA-mir-451* mildly accumulate the hairpin precursor, but mAgo2 complexes strictly contain cleaved and matured forms of miR-451. (e) mAgo2 was not stabilized by *tRNA-mir-451-CM*, compared to *tRNA-mir-451*. (f) Luciferase sensor assays in *Drosophila* S2 cells. Sensor constructs were empty, or contained complementary sites to miR-276a-5p or miR-276a-3p. Tests were done in quadruplet for each sample. Error bars represent standard variation. Student's two-tailed, equal variance t-test was performed. (g) S2 cells were depleted of miRNA biogenesis factors using the indicated dsRNAs or control *GFP* dsRNA. Transfection of scrambled siRNA duplex mildly improved AGO1 accumulation, but synthetic miR-276a-miR-276a* duplex induced robust recovery of AGO1 levels. See also Fig. S6.